J Fluoresc (2011) 21:17–24
DOI 10.1007/s10895-010-0685-2

ORIGINAL PAPER

Spectroscopic Studies on the Thermodynamics of L-Cysteine Capped CdSe/CdS Quantum Dots—BSA Interactions

Ling Ding · P. J. Zhou · S. Q. Li · G. Y. Shi · T. Zhong · M. Wu

Received: 4 February 2010 / Accepted: 1 June 2010 / Published online: 1 July 2010

Abstract CdSe/CdS quantum dots (QDs) capped with L-cysteine can provide an effective platform for the interactions with bovine serum albumin (BSA). In this study, absorption and fluorescence (FL) spectroscopy were used to study the binding reactions of QDs with BSA, respectively. The binding constant ($\approx 10^4$ M^{-1}) from FL quenching method matches well with that determined from the absorption spectral changes. The modified Stern-Volmer quenching constant (5.23×10^4, 5.22×10^4, and 4.90×10^4 M^{-1}) and the binding sites ($\approx$1) at different temperatures (304 K, 309 K, and 314 K) and corresponding thermodynamic parameters were calculated ($\Delta G<0$, $\Delta H<0$, and $\Delta S<0$). The results show the quenching constant is inversely correlated with temperature. It indicates the quenching mechanism is the static quenching in nature rather than dynamic quenching. The negative values of free energy ($\Delta G<0$) suggest that the binding process is spontaneous, $\Delta H<0$ and $\Delta S<0$ suggest that the binding of QDs to BSA is enthalpy-driven. The enthalpy and entropy changes for the formation of ground state complex depend on the capping agent of QDs and the protein types. Furthermore, the reaction forces were discussed between QDs and BSA, and the results show hydrogen bonds and van der Waals interactions play a major role in the binding reaction.

L. Ding · P. J. Zhou (✉) · S. Q. Li · G. Y. Shi
College of Resource & Environmental Sciences,
Hubei Biomass-Resource Chemistry and Environmental Biotechnology Key Laboratory, Wuhan University,
Wuhan 430079, People's Republic of China
e-mail: zhoupj@whu.edu.cn
e-mail: zhoupjg@gmail.com

L. Ding · T. Zhong · M. Wu
College of Chemical Engineering and Technology,
Wuhan University of Science and Technology,
Wuhan 430081, People's Republic of China

Keywords CdSe/CdS · Quantum dots · Bovine serum albumin · Spectroscopic methods · Thermodynamic parameters

Introduction

Due to the quantum confinement of their electronic states, quantum dots (QDs) have gained a lot of attention in recent years. In comparison with conventional fluorescent markers (e.g., organic dyes and fluorescent proteins), QDs have broad excitation spectra, sharp emission, and easily tunable emission properties [1–7]. Thus, they are becoming favored for robust fluorescent probes in biological applications [4, 5, 8–10]. Particularly, water-soluble and biological-compatible QDs have played an important role in a wide range of applications in biotechnology, medicine and other fields [11–14]. Hence, a number of surface functionalization schemes have been developed to make QDs water soluble and biological-compatible and suitable for use in cell biology and immunoassay etc. Since Alivisatos [4] and Nie [5] coupled biomacromolecules to the surface of QDs, it opened up a new age in applications of biology and medicine.

As we known, QDs can be combined with proteins in vivo and thus impact the structure and function of protein. Though there are a lot of researches on the interaction of QDs with protein, e.g., Kotov [15] and Nyokong [16] studied the bioconjugation between QDs and bovine serum albumin (BSA) by using the crosslinker; Guldi and co-workers [17] probed human serum albumin (HSA) and its interaction with QDs by electrostatic interactions; Those studies just stay on the surface level and a few studies investigated the response of biological systems to QDs in detail. Renganathan etc [18] have further studied the interaction QDs with BSA by the methods of UV-visible,

and synchronous fluorescence (FL) spectroscopic measurements and gained the apparent association constant and the degree of association, but they did not investigate the interaction forces between them. Although Liu's group[19] used various spectroscopic (FL, Circular Dichroism (CD)) techniques to gain the thermodynamic parameters (ΔH, ΔG and ΔS) of the reaction between QDs and HAS at different temperatures and they found electrostatic interactions play a major role in stabilizing the complex (QDs-HSA), factors that determine the mode of the interaction of them are still unclear at present. Therefore, it is necessary to continue to study the interaction between QDs and protein for further investigating the biological effects of QDs.

In this report, we choose BSA as our protein model because of its medicinal importance, low cost, ready availability, and unusual ligand-binding properties [20–23]. L-cysteine-capped CdSe/CdS (following abbreviated: QDs) are selected as the protein receptor and the QDs-BSA interactions are explored by using UV and FL spectroscopic techniques. The thermodynamic parameters (ΔH, ΔG and ΔS) obtained from spectroscopic techniques studies, which indicate an enthalpy driven process, revealed dramatic differences when compared with other results. We demonstrated hydrogen bonds and van der Waals interactions, which relate with the type of the surface of capping agent and protein, play a major role in the binding reaction between BSA and QDs.

Experimental section

Materials

L-cysteine, cadmium chloride ($CdCl_2$), selenium (Se), sodium borohydride ($NaBH_4$), ethanol (C_2H_5OH), sodium hydroxide (NaOH), Sodium sulfide (Na_2S) Tris (hydroxymethyl) aminomethane, bovine serum albumin (BSA), and other routine chemicals were purchased from Shenshi Chem. Ltd. All the chemicals used were of analytical grade and double distilled deionized water was used in all experiments.

Instrumental

All FL measurements were recorded using a RF-5301 (Shimadzu) and F-2500(Hitachi) fluorometers. A Lambda 35 (PerkinElmer) Spectrophotometer was used with a cell of 1.0 cm path length.

Preparation of L-cysteine capped CdSe/CdS QDs

The preparation of L-cysteine capped CdSe/CdS QDs followed by the modified method was adopted from literature.[24] Briefly, 0.3 mmol Se and 0.3 mmol $NaBH_4$ were added into a 100 mL round bottom flask (I). 10 ml C_2H_5OH was also added into this flask and purged with pure nitrogen gas for at least 30 min with magnetic stirring, and then heated at 40 °C for 30 min (reaction 1). Meanwhile, 20 mL 0.02 mol/L $CdCl_2$, 0.0012 mol L-cysteine ($n_{L\text{-}Cysteine}/n_{Cd}=3$) and 0.1 mol/L NaOH (pH=10.50) were added into another 100 mL round bottom flask (II) which was also purged and stirred (vide supra) (reaction 2). The solution in flask (I) was pressed into flask (II) by the pressure of N_2 with a rubber tube after 30 min, and then the flask (II) was sealed, refluxed, and maintained at 90 °C(reaction 3). After 60 min, 8 mL 0.9 mmol/L Na_2S was titrated and then this reaction was kept 45 °C for 60 min. The L-cysteine capped CdSe/CdS QDs were obtained through ethanol precipitation with centrifugation at 4,000 rpm for 5 min, these QDs was treated with ethanol in three repeated cycles to remove the contaminant. Finally, these QDs were dissolved in Tris-HCl buffer solution and stored at 277 K.

Methods

A 2 mL solution, containing appropriate concentration of QDs was added with 10^{-5} M BSA solution and mixed. UV-visible spectra of all solutions were recorded in the range of 200–800 nm.

A known concentration of QDs in Tris-HCl buffer solution was added into 10^{-5} M BSA solution and mixed at different temperatures. The fluorescent intensity of the solution was recorded at excitation wavelength of 280 nm by using F-2500 fluorometer, and the slit widths used for excitation and emission were 5 nm, respectively. And then 10^{-5} M BSA solution was added into QDs solution and the excitation wavelength was 360 nm by using RF-5301 fluorometer, and the slit widths used for excitation and emission were 5 nm.

Results and discussion

Characterization of QDs

The absorption (a) and FL (b) spectra of QDs were presented in Fig. 1 to identify the presence of nanoparticles. The absorption spectra showed the formation of QDs particles having absorption in the range of less than about 525 nm. Comparing to the bulk species, there is a blue shift in the absorbance spectrum [25], which can be explained by the fact that quantum confinement effects determine the optical properties of QDs and the degree of electronic confinement is highly correlated with particle size [26]. The sample exhibits the emission peak at about 564 nm (Fig. 1b) and this spectrum indicates the well-proportioned

size distribution of the particles. A good overlap of emission of BSA on the absorption of QD was observed in Fig. 1. After binding reaction, QD is so close to the residues of BSA that molecular resonance energy transfer occurs between them.

Effect of QDs on BSA absorption spectra

Absorption spectra can not only distinguish between dynamic quenching and static quenching, but also obtain the binding constant (K) of the reaction [18, 27]. The absorption spectra of BSA in absence and presence of QDs at room temperature (299 K) is shown in Fig. 2. The addition of QDs led to a gradual increase in the absorption intensity of BSA with a blue shift of 2 nm (278 nm→276 nm). However, our previous study showed CdSe QDs led to a minor decrease in the absorption intensity of BSA with the appearance of the isoabsorptive point [24]. Other similar studies [16, 18, 28] about the interaction between BSA with QDs and TiO_2 were also reported. As we known, dynamic quenching will not change the absorption spectra because it only affects the excited state of fluorophore; as ground state complex formation, static quenching often lead to change in the absorption spectra [27]. Therefore, the above results suggest there are the ground state complex formation between BSA and QDs. The blue shift of absorption spectra implies the structure of BSA is changed possibly [18].

There are the equilibrium is defined by Eqs. 1 and 2 for the complex formation between BSA and QDs,

$$\mathrm{BSA} + \mathrm{QDs} \underset{\longleftarrow}{\overset{K_{\mathrm{app}}}{\longrightarrow}} \mathrm{BSA} - - - \mathrm{QDs} \tag{1}$$

$$K_{\mathrm{app}} = \frac{[\mathrm{BSA} - - - \mathrm{QDs}]}{[\mathrm{BSA}] \cdot [\mathrm{QDs}]} \tag{2}$$

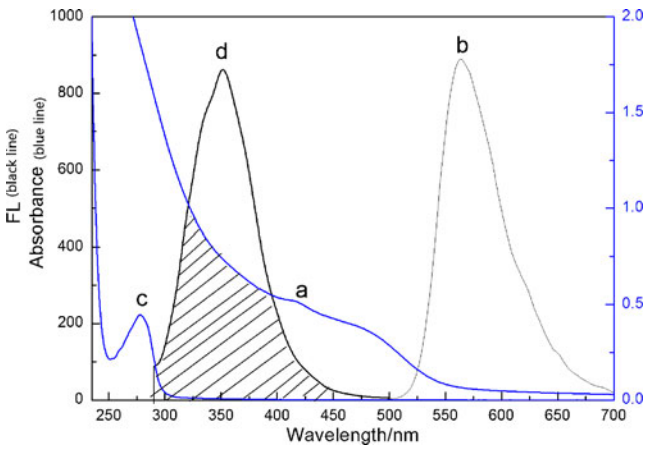

Fig. 1 Absorption and emission spectras of QDs **a** and **b** and BSA **c** and **d** respectively

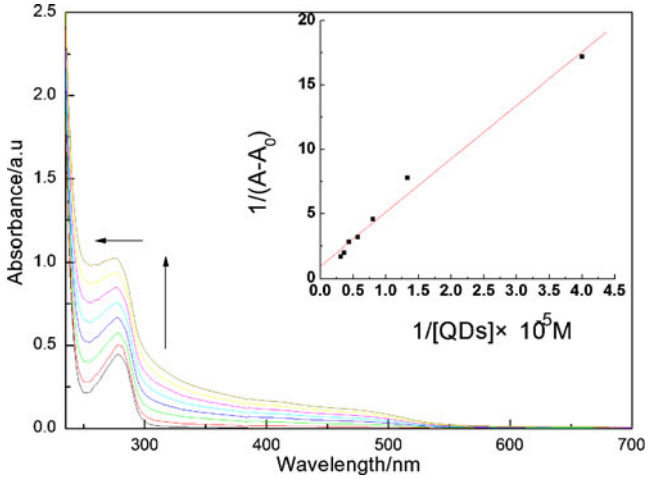

Fig. 2 Absorption spectrum of BSA in the presence of QDs in the concentration range of $(0–3)\times10^{-5}$M

where K_{app} is the apparent association constant. K_{app} can be obtained by the changes of the intensity of absorption [18, 28, 29] and expressed as Eq. 3,

$$\frac{1}{A - A_0} = \frac{1}{A_C - A_0} + \frac{1}{K_{\mathrm{app}}(A_C - A_0)[\mathrm{QDs}]} \tag{3}$$

where A, A_0, A_c are the absorbance of BSA containing different concentrations of QDs, BSA and the complex, respectively. The values of $(A-A_0)^{-1}$ were calculated and plotted against quencher concentration $[\mathrm{QDs}]^{-1}$ according to Eq. 3 as shown in the inset of Fig. 2. After linear fit, the slope equals to the value of $\left(K_{\mathrm{app}}(A_C - A_0)\right)^{-1}$ and the intercept is $(A_C-A_0)^{-1}$ on the ordinate. The calculated value of K_{app} is about 2.38×10^4 M^{-1} (R=0.9931).

FL quenching studies

Effect of QDs on BSA FL spectra

Figure 3 is FL spectra of BSA with various concentrations (mol/L) of QDs at 304 K, 309 K, 314 K, respectively. The observed FL band centered about 350 nm. The FL intensity was significantly quenched by the addition of QDs at different temperatures when the concentration of BSA is 10^{-5} M. Because the emission wavelengths of QDs are much far away from the BSA absorption and emission, so the emission of QDs between 290–450 nm are not considered. The result suggests the interaction between BSA and QDs occur and quenching effect of QDs on the FL emission of BSA is found to be concentration dependent, that is, QDs can bind to the BSA.

The quenching FL is known to occur by excited state reactions, energy transfer, collisional quenching (dynamic quenching) and complex formation (static quenching) [27].

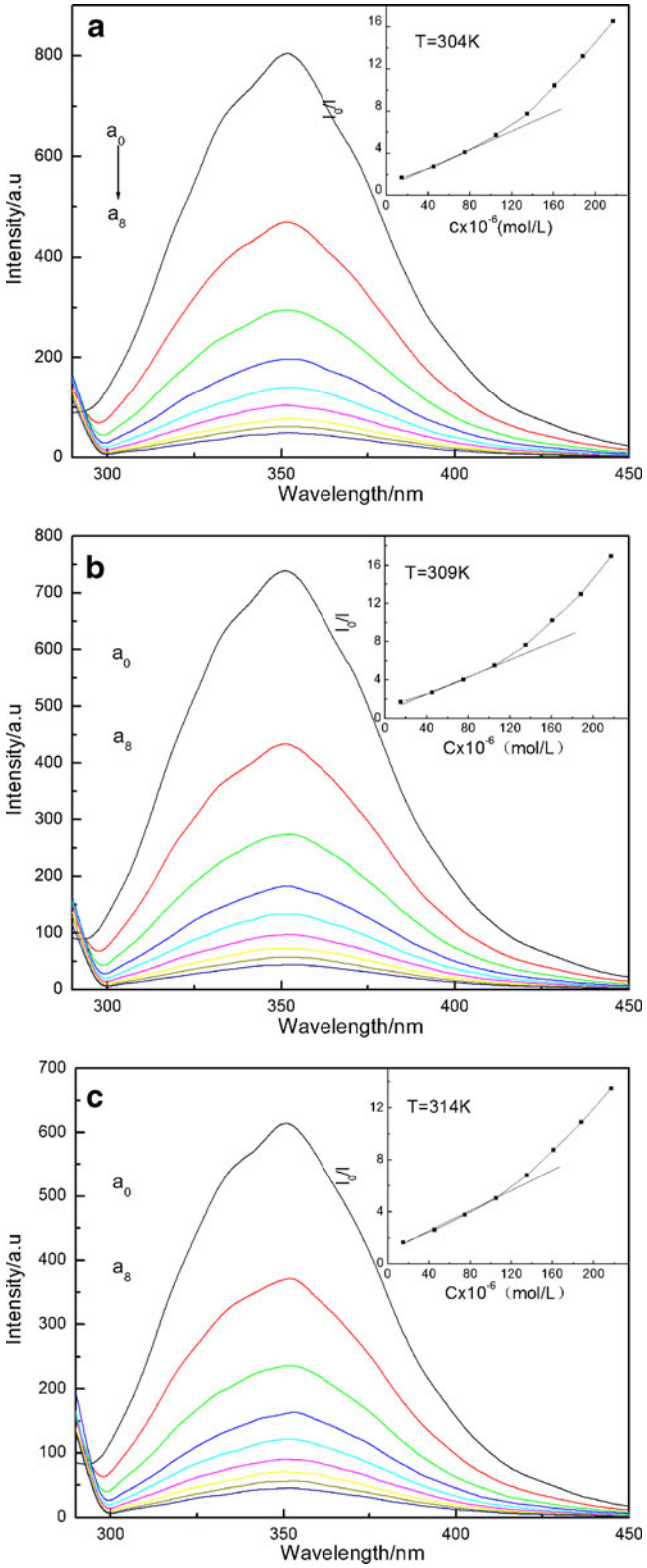

Fig. 3 Fluorescence emission spectra of BSA in the presence of different concentrations of QDs obtained in Tris–HCl buffer solution, and the inset corresponds to Stern-Volmer plots of the quenching of the fluorescence of BSA by QDs at different temperatures (**a** 304 K, **b** 309 K, **c** 314 K)

The last two processes are mainly considered. Both dynamic quenching and static quenching reveal the connection of linearity between relative FL intensity (I_0/I) and QDs concentration. The quenching of BSA FL by QDs can be described by a Stern-Volmer equation:

$$\frac{I_0}{I} = 1 + K_{sv}[Q] \tag{4}$$

where I_0 and I are the FL intensity of BSA in the absence and presence of QDs respectively, [Q] is the QDs concentration and K_{sv} is the Stern-Volmer quenching constant. Inset of Figure 3 shows that the results agree with the Stern-Volmer equation excellently at low concentrations (1.5×10^{-6}–1.05×10^{-5} M) and the results depart from the initial linearity at higher concentration.

The ratios I_0/I were calculated and plotted against quencher concentration according to Eq. 4 at low concentrations at different temperatures. After linear fit, K_{sv} were calculated from the slope of the plots and the correlation coefficient in the Table 1. The results show the quenching constant K_{sv} are various at different temperatures, at the same time, K_{sv} is inversely correlated with temperature. As we known, dynamic quenching depends on diffusion, and the coefficient of diffusion will augment because of the increase of temperature, so the quenching constant is directly correlated with temperature; moreover, for the static quenching, the stability of complex formation will descend because of the increase of temperature, so the quenching constant is inversely correlated with temperature. Therefore, this proves that the quenching mechanism is the static quenching in nature rather than dynamic quenching.

According to dimolecular quenching equation:

$$K_{sv} = K_q \cdot \tau_0 \tag{5}$$

Where K_q is dimolecular rate constant and τ_0 (10^{-8} s) is the average lifetime of the FL substance without quencher [27]. Therefore, according to Eq. 5, K_q were calculated as shown in Table 1. Generally, quenching on the biological macromolecules of the large diffusion and collision constant is 10^{10} $M^{-1}\cdot s^{-1}$. Thus, K_q is about two orders higher than 10^{10} $M^{-1}\cdot s^{-1}$. Those results also indicate the present static quenching of the FL in the mechanism of interaction.

Both temperature and dimolecular quenching prove that the quenching mechanism of a QDs-BSA binding reaction is static quenching. Therefore, the quenching data were analyzed according to the modified Stern-Volmer equation [30]:

$$\frac{F_0}{\Delta F} = \frac{1}{f_a K_a}\frac{1}{[Q]} + \frac{1}{f_a} \tag{6}$$

Table 1 Stern-Volmer and modified Stern-Volmer quenching constants of the QDs-BSA system at different temperatures

T/K	Stern-Volmer method			Modified Stern-Volmer method	
	K_{sv}/L·mol^{-1}	R	K_q/ M^{-1}·s^{-1}	K_a/L·mol^{-1}	R
304	5.12×10^4	0.9943	5.12×10^{12}	5.23×10^4	0.9962
309	4.58×10^4	0.9963	4.58×10^{12}	5.22×10^4	0.9963
314	3.81×10^4	0.9976	3.81×10^{12}	4.90×10^4	0.9973

Where, ΔF is the difference in FL in the absence and presence of quencher at concentration $[Q]$, f_a is the mole fraction of solvent-accessible fluorophore, and K_a is the effective quenching constant for the accessible fluorophores, which are analogous to apparent binding constants for the system of quencher-acceptor [31]. The ratios $\frac{F_0}{\Delta F}$ were calculated and plotted against quencher concentration $[Q]^{-1}$ according to Eq. 6 at different temperatures as shown in Fig. 4. After linear fit, the slope equals to the value of $(f_aK_a)^{-1}$ and the intercept is f_a^{-1} on the ordinate. So K_a were calculated at different temperatures according to the slope $(f_aK_a)^{-1}$ and the intercept $\left(f_a^{-1}\right)$ as shown in Table 1. K_a is also inversely correlated with temperature and it agrees with K_{sv}'s dependence on temperature. This is also indicates that the quenching mechanism is the static quenching (complex formation).

Binding sites and binding constant

Because of the mechanism of static quenching, there may be binding sites in the BSA; the binding sites can be deduced from the relationship between fluorophore (BSA) and quencher (QDs). According to the Renganaathan's group [18, 32], the binding sites and binding constant can be calculated from the following equation:

$$n\mathrm{Q} + \mathrm{B} \overset{K}{\rightleftharpoons} \mathrm{Q}_n \cdots \mathrm{B} \tag{7}$$

Where B is the fluorophore (BSA), Q is the quencher (QDs), and $\mathrm{Q}_n \cdots \mathrm{B}$ is the postulated complex between one molecule of BSA and n QDs. So the constant K is given by

$$K = \frac{[\mathrm{Q}_n \cdots \mathrm{B}]}{[\mathrm{Q}]^n \cdot [\mathrm{B}]} \tag{8}$$

Where [B] and [Q] are the concentration of unbound BSA and QDs, respectively, and $[\mathrm{Q}_n \cdots \mathrm{B}]$ is the concentration of the postulated complex $(\mathrm{Q}_n \cdots \mathrm{B})$. If $[\mathrm{B}_0]$ is the overall concentration of BSA, then Eq. 9 is concluded,

$$[\mathrm{B}_0] = [\mathrm{Q}_n \cdots \mathrm{B}] + [\mathrm{B}] \tag{9}$$

As we known, the relationship between FL intensity and the unbound BSA is expressed as:

$$\frac{[\mathrm{B}]}{[\mathrm{B}_0]} = \frac{F}{F_0} \tag{10}$$

where F_0 and F are the FL intensity of BSA in the absence and presence of QDs, respectively. Combining Eq. 8 with Eq. 9, the relationship (Eq. 11) between FL intensity and the concentration of QDs can be concluded.

$$\log\left[\frac{F_0 - F}{F}\right] = \log K + n\log[\mathrm{Q}] \tag{11}$$

where K is the binding constant and n are the numbers of binding sites between BSA and QDs. The values of $\log\left[\frac{F_0-F}{F}\right]$ were plotted against log[Q] according to Eq. 11 at different temperatures as shown in Fig. 5. After linear fit, n and K were calculated at different temperatures according to the slope n and the intercept log K as shown in Table 2. K is also inversely correlated with temperature and it agrees with the dependence on temperature of K_a, at the same time, n is also inversely correlated with temperature. The values of binding constant obtained from this method agree with that obtained from the modified Stern-Volmer equation at different temperatures, that is, the values of binding constant all are about 10^4 L·mol^{-1} for sure. The good agreement indicates there are reaction between BSA and QDs and the quenching mechanism is the static quenching

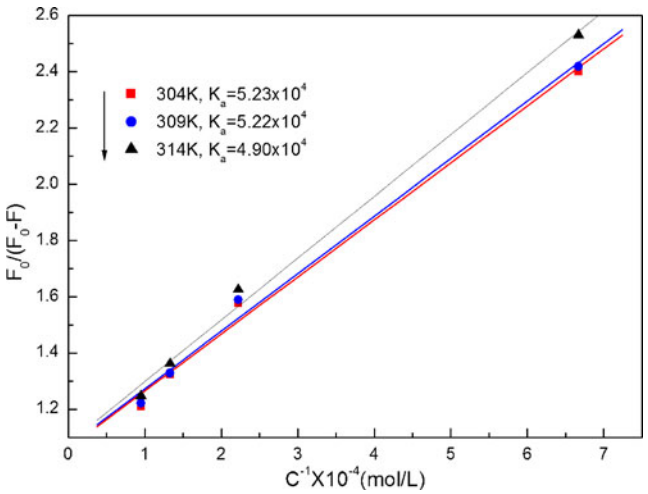

Fig. 4 Modified Stern-Volmer plots of QDs concentration dependence of FL intensity of BSA with the best correlation coefficient at different temperatures

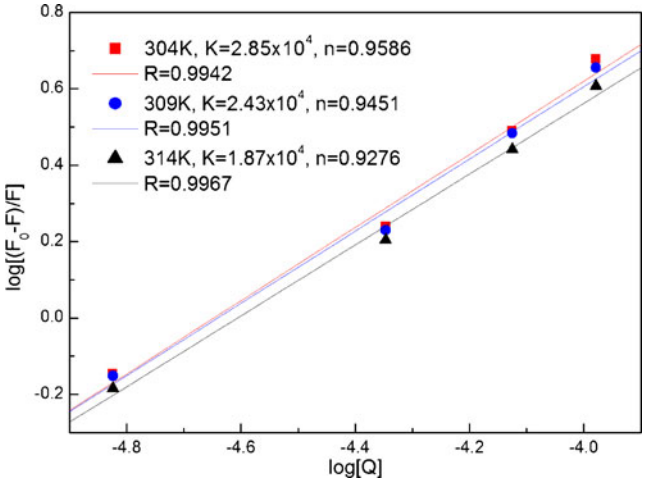

Fig. 5 The plot of log $[(F_0\text{-}F)/F]$ versus log [Q] for BSA with QDs

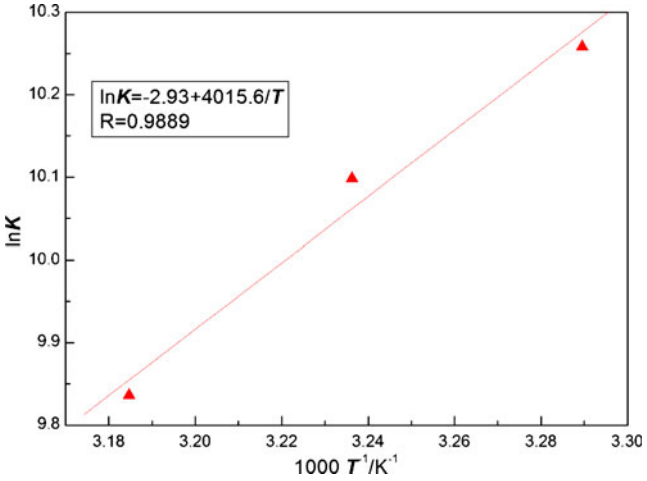

Fig. 6 Van't Hoff plots of BSA-QDs system

(complex formation). The number of binding site is close to 1 at different temperatures, and other authors' results also revealed *n* is about 1, this implies there is only one type of interaction between BSA and QDs.

The thermodynamic study

The binding constant (*K*) were calculated at different temperatures as shown in Table 2. Therefore, the thermodynamic parameters were calculated by using the van't Hoff equation (Eq. 12).

$$\ln K = -\frac{\Delta H}{RT} + \frac{\Delta S}{R} \tag{12}$$

Where ΔH and ΔS are the standard enthalpy and entropy change for the reaction, respectively, R is the gas constant and T is temperature. This equation assumes enthalpy and entropy are temperature independent in the temperature range studied [19, 33]. The values of ln K were plotted against T^{-1} according to Eq. 12 at different temperatures as shown in Fig. 6. It can be seen from Fig. 6 there was a best-fit straight line (correlation coefficient R= 0.9889). ΔH and ΔS were calculated at different temperatures according to the slope $-\frac{\Delta H}{R}$ and the intercept $\frac{\Delta S}{R}$ as shown in Table 2. Using the relationship $\Delta G = \Delta H - T\Delta S$, the free energy change (ΔG) is then estimated as also shown in Table 2.

From the point of thermodynamics, all the chemical, physical, biological process are accompanied by the change of thermodynamic parameters [34, 35]. For example, the free energy (ΔG) determine whether a reaction can take place spontaneous; the changes of enthalpy (ΔH) can be considered as an indicator of the increase of intermolecular bond energies in binding process; while the entropy changes (ΔS) reflect the change of disorder of the system during the reaction [34, 35]. Table 2 shows the values of ΔG, ΔH and ΔS (ΔG<0, ΔH<0, ΔS<0), the negative values of free energy (ΔG<0) suggest that the binding process is spontaneous, ΔH<0 and ΔS<0 suggest that the binding of QDs to BSA is enthalpy-driven. The values of ΔG, ΔH and ΔS reveal that the reaction of QDs with BSA feature a favorable enthalpy change (ΔH<0) [36], which is offset partially by unfavorable entropy loss (ΔS<0), affording overall free energy changes (ΔG).

As we known, the interaction between endogenous or exogenous ligands and biological macromolecules is a complex process that involves not only electrostatic interactions, multiple hydrogen bonds, van der Waals interactions, but also hydrophobic and π-π stacking [36, 37]. Ross and his co-worker [38] thought electrostatic interactions are important if ΔH is negative; and ΔS<0 is the role of hydrogen bond and van der Waals interactions' common characteristics. These results indicate that hydrogen bonds and van der Waals interactions play a major role in the binding reaction between BSA and QDs, but the electrostatic interactions are also important.

The binding constant (*K*) can be calculated according to Eq. 12 between BSA and QDs at room temperature

Table 2 Thermodynamic parameters and the number of binding sites of QDs-BSA at different temperatures

T/K	*K*/L·mol^{-1}	ΔH/kJ·mol^{-1}	ΔG/kJ·mol^{-1}	ΔS/J·mol^{-1}·K^{-1}	*R*	*n*
304	2.85×10^4	-33.39	-25.98	-24.36	0.9889	0.9586
309	2.43×10^4		-25.86			0.9451
314	1.87×10^4		-25.74			0.9276

(299 K), and K is about $3.63\times10^{4}M^{-1}$. The value of K matches well with the apparent association constant $\left(K_{app}=2.38\times10^{4}M^{-1}\right)$ obtained from the absorbance spectra at 299 K. The good agreement between K and K_{app} suggests there are the association (reaction) between BSA and QDs. The validity of this association is proved further by FL spectra at low concentrations (from 1.5×10^{-6}–1.05×10^{-5} M). In other words, the ground state complex was formed. The mode of this binding reaction is obtained from the changes of the thermodynamic parameters (ΔH, ΔG and ΔS). Liu's results showed the electrostatic interactions played a major role in the reaction, because the electrostatic interactions occurred between the negatively charged QDs and the cationic "hot spot" around the active site of protein (human serum albumin, HSA). Other report [18, 36, 39] also studied the interaction between nanoparticles (NPs) and proteins, and showed both the capping agent of NPs and protein played an important role in the interaction. Our results suggest hydrogen bonds and van der Waals interactions play a major role in the binding reaction between BSA and QDs. Structurally, this is due to the existence of $-NH_2$ in the capping agent (L-cysteine, Isoelectric Point (pI)=5.02), so more hydrogen bonds can be easily formed between QDs and BSA, and van der Waals interactions are also existence. Besides, the electrostatic interactions should not be ignored. The electrostatic attraction is caused by positive charge of BSA and negative charge of QD. Though BSA is negatively charge (pI=4.7) in this solution, BSA and HSA have similar binding sites and high degree of homology [40, 41]. Thus, BSA also has the cationic "hot spot" around the active site for formation of the electrostatic interactions between QDs and BSA. At the same time, the electrostatic interactions may be formed between the negatively charged BSA and the positively charged QDs because the excess cationic (Cd^{2+}) is absorbed on the surface of QDs. It is particularly noteworthy that we did not consider their difference between BSA and HSA for their high degree of homology. The interaction from strong to weak force is electrostatic, H-bonding and Van der Wall in sequence.

Conclusions

In this study, the interactions between L-cysteine-capped CdSe/CdS QDs and BSA have been studied by absorption and fluorescence spectroscopy. The results clearly indicated that QDs quenches the fluorescence of BSA through the formation of ground state complex which is confirmed by all spectra. Both the thermodynamic parameters and number of the binding sites were calculated according to the relevant fluorescence data. The binding constants, which were gained according to absorption and fluorescence spectra data respectively, were very consistent. Those results showed hydrogen bonds and van der Waals interactions play a major role in the binding reaction between them, and the reaction of QDs with BSA feature a favorable enthalpy change. Comparing with previous studies, we can find QDs-BSA interactions provide drastically different thermodynamic parameters that depend on both the capping agent of QDs and the protein type.

Acknowledgement We gratefully acknowledge the financial support of the National High-Tech Research and Development Program of China (863 Program, 2007AA06Z418) and National Natural Science Foundation of China (20577036, 20777058, 20977070).

References

1. Brus LE (1983) A simple model for the ionization potential, electron affinity, and aqueous redox potentials of small semiconductor crystallites. J Chem Phys 79:5566. doi:10.1063/1.445676
2. Ceo S, Woo WK, Bawendi M, Bulovic V (2002) Electroluminescence from single monolayers of nanocrystals in molecular organic devices. Nature 420:800–803. doi:10.1038/nature01217
3. El-Sayed MA (2004) Small is different: shape-, size-, and composition-dependent properties of some colloidal semiconductor nanocrystals. Acc Chem Res 37:326–333. doi:10.1021/ar020204f
4. Jr M, Bruchez MM, Gin P, Weiss S, Alivisatos AP (1998) Semiconductor nanocrystals as fluorescent biological labels. Science 281:2013–2016. doi:10.1126/science.281.5385.2013
5. Chan WCW, Nie S (1998) Quantum dot bioconjugates for ultrasensitive nonisotopic detection. Science 281:2016–2018. doi:10.1126/science.281.5385.2016
6. Wu FX, Lewis JW, Kliger DS, Zhang JZ (2003) Unusual excitation intensity dependence of fluorescence of CdTe nanoparticles. J Chem Phys 118:12. doi:10.1063/1.1533733
7. Zhong XH, Feng YY, Knoll W, Han M (2003) Alloyed $Zn_xCd_{1-x}S$ nanocrystals with highly narrow luminescence spectral width. J Am Chem Soc 125:13559–13563. doi:10.1021/ja036683a
8. Mahtab R, Rogers JP, Murphy CJ (1995) Protein-sized quantum dot luminescence can distinguish between "straight", "bent" and "kinked" oligonucleotides. J Am Chem Soc 117:9099–9100. doi:10.1021/ja00140a040
9. Mahtab R, Rogers JP, Singleton CP, Murphy CJ (1996) Preferential adsorption of a "kinked" DNA to a neutral curved surface: comparisons to and implications for nonspecific DNA-protein interactions. J Am Chem Soc 118:7028–7032. doi:10.1021/ja961602e
10. Mattoussi H, Mauro JM, Goldman ER, Anderson GP, Sundar VC, Mikulec FV, Bawendi MG (2000) Self-assembly of CdSe-ZnS quantum dot bioconjugates using an engineered recombinant protein. J Am Chem Soc 122:12142–12150. doi:10.1021/ja002535y
11. Gaponik N, Radtchenko IL, Sukhorukov GB, Weller H, Rogach AL (2002) Toward encoding combinatorial libraries: charge-driven microencapsulation of semiconductor nanocrystals luminescing in the visible and near IR. Adv Mater 14:879–882. doi:10.1002/1521-4095(20020618)14:12>879::AID-ADMA879&lt:3.0.CO;2-A

12. Talapin DV, Rogach AL, Shevchenko EV, Komowski A, Haase M, Weller H (2002) Dynamic distribution of growth rates within the ensembles of colloidal II–VI and III–V semiconductor nanocrystals as a factor governing their photoluminescence efficiency. J Am Chem Soc 124:5782–5790. doi:10.1021/ja0123599
13. Samia ACS, Chen X, Burda C (2003) Semiconductor quantum dots for photodynamic therapy. J Am Chem Soc 125:15736–15737. doi:10.1021/ja0386905
14. Samia ACS, Dayal S, Burda C (2006) Quantum dot-based energy transfer:perspectives and potential for applications in photodynamic therapy. Photochem Photobiol 82:617–625. doi:10.1562/2005-05-11-IR-525
15. Mamedova NN, Kotov NA, Rogach AL, Studer J (2001) Albumin-CdTe nanoparticle bioconjugates:preparation, structure, and interunit energy transfer with antenna effect. Nano Lett 1:281–286. doi:10.1021/nl015519n
16. Idowu M, Lamprecht E, Nyokong T (2008) Interaction of water-soluble thiol capped CdTe quantum dots and bovine serum albumin. J Photochem Photobiol A: Chem 198:7–12. doi:10.1016/j.jphotochem.2008.02.008
17. Gerhards C, Schulz-Drost C, Sgobba V, Guldi DM (2008) Conjugating luminescent CdTe quantum dots with biomolecules. J Phys Chem B 112:14482–14491. doi:10.1021/jp8030094
18. Jhonsi MA, Kathiravan A, Renganathan R (2009) Spectroscopic studies on the interaction of colloidal capped CdS nanoparticles with bovine serum albumin. Colloid Surface B 72:167. doi:10.1016/j.colsurfb.2009.03.030
19. Xiao Q, Huang S, Qi ZD, Zhou B, He ZK, Liu Y (2008) Conformation, thermodynamics and stoichiometry of HSA adsorbed to colloidal CdSe/ZnS quantum dots. Biochim Biophys Acta, Proteins Proteomics 1487:1020–1027. doi:10.1016/j.bbapap.2008.03.018
20. Olson RE, Christ DD (1996) Plasma protein binding of drugs. Ann Rep Med Chem 31:327–336. doi:10.1016/S0065-7743(08)60472-8
21. Xie J, Zheng Y, Ying JY (2009) Protein-directed synthesis of highly fluorescent gold nanoclusters. J Am Chem Soc 131:888–889. doi:10.1021/ja806804u
22. Yang L, Xing R, Shen Q, Jiang K, Ye F, Wang J, Ren Q (2006) Fabrication of protein-conjugated silver sulfide nanorods in the bovine serum albumin solution. J Phys Chem B 110:10534–10539. doi:10.1021/jp055603h
23. Xie JP, Lee JY, Wang DIC (2007) Synthesis of single-crystallinegold nanoplates in aqueous solutions through biomineralization by serum albumin protein. J Phys Chem C 111:10226–10232. doi:10.1021/jp0719715
24. Liu P, Wang QS, Li X (2009) Studies on CdSe/l-cysteine quantum dots synthesized in aqueous solution for biological labeling. J Phys Chem C 113:7670–7676. doi:10.1021/jp901292q
25. Henglein A (1989) Small-particle research:physicochemical properties of extremely small colloidal metal and semiconductor particles. Chem Rev 89:1861–1873. doi:10.1021/cr00098a010
26. M. K. Gattas-Asfura, R. M. Leblanc, (2003), Peptide-coated CdS quantumn dots for the optical detection of copper(I) and silver(II). *Chem. Commun.* 2684–2685. doi:10.1039/b308991f
27. Lakowicz JR (2006) Principles of fluorescence spectroscopy, 3rd edn. Springer, New York
28. Kathiravan A, Renganathan R (2008) Interaction of colloidal TiO_2 with bovine serum albumin: a fluorescence quenching study. Colloid Surface A 324:176–180. doi:10.1016/j.colsurfa.2008.04.017
29. Benesi HA, Hildebrand JH (1949) A Spectrophotometric investigation of the interaction of iodine with aromatic hydrocarbons. J Am Chem Soc 71:2703–2707. doi:10.1021/ja01176a030
30. Lehrer SS (1971) Solute perturbation of protein fluorescence. The quenching of the tryptophyl fluorescence of model compounds and of lysozyme by iodide ion. Biochemistry 10:3254–3263. doi:10.1021/bi00793a015
31. Pu L (2004) Fluorescence of organic molecules in chiral recognition. Chem Rev 104:1687–1716. doi:10.1021/cr030052h
32. Anbazhagan V, Renganathan R (2008) Study on the binding of 2, 3-diazabicyclo[2.2.2]oct-2-ene with bovine serum albumin by fluorescence spectroscopy. J Lumin 128:1454. doi:10.1016/j.jlumin.2008.02.004
33. Mahtab R, Harden HH, Murphy CJ (2000) Temperature- and salt-dependent binding of long DNA to protein-sized quantum dots: thermodynamics of "inorganic protein"–DNA interactions. J Am Chem Soc 122:14. doi:10.1021/ja9907156
34. Cestaria AR, Vieiraa EFS, Simonib JA, Airoldi C (2000) Thermochemical investigation on the adsorption of some divalent cations on modified silicas obtained from sol-gel process. Thermochim Acta 348:25–31. doi:10.1016/S0040-6031(99)00380-9
35. Liu P, Wang QS, Li X, Zhang CC (2009) Zeta-potentials and enthalpy changes in the process of electrostatic self-assembly of cations on silica surface. Powder Technol 193:46–49. doi:10.1016/j.powtec.2009.02.006
36. De M, You CC, Srivastava S, Rotello VM (2007) Biomimetic interactions of proteins with functionalized nanoparticles: a thermodynamic study. J Am Chem Soc 129:10747–10753. doi:10.1021/ja071642q
37. Leckband D (2000) Measuring the forces that control protein interactions. Annu Rev Biophys Biomol Struct 29:1–26. doi:10.1146/annurev.biophys.29.1.1
38. Ross DP, Subramanian S (1981) Thermodynamics of protein association reactions: forces contributing to stability. Biochemistry 20:3096–3102. doi:10.1021/bi00514a017
39. Qi K, Ma QG, Remsen EE, Clark CG, Wooley KL (2004) Determination of the bioavailability of biotin conjugated onto shell cross-linked (SCK) nanoparticles. J Am Chem Soc 126:6599–6607. doi:10.1021/ja039647k
40. Carter DC, Ho JX (1994) Structure of Serum Albumin. Adv Pro Chem 45:153–176. doi:10.1016/S0065-3233(08)60640-3
41. Peters T (1985) Serum albumin. Adv Pro Chem 37:161–245. doi:10.1016/S0065-3233(08)60065-0